Electronic Supporting Information

The First Example of a Zirconium-Oxide Based Metal-Organic Framework Constructed from Monocarboxylate Ligands

Weibin Liang,[a] Ravichandar Babarao,[b] Michael J. Murphy[a] and Deanna M. D'Alessandro[a]*

[a]School of Chemistry, The University of Sydney, New South Wales 2006, Australia.
[b]CSIRO Division of Materials Science and Engineering, Private Bag 33, Clayton South MIDS, Victoria 3169, Australia.

Table of Contents

S1. Brief summary of Zirconium-oxide based Metal-Organic Frameworks[1-18]

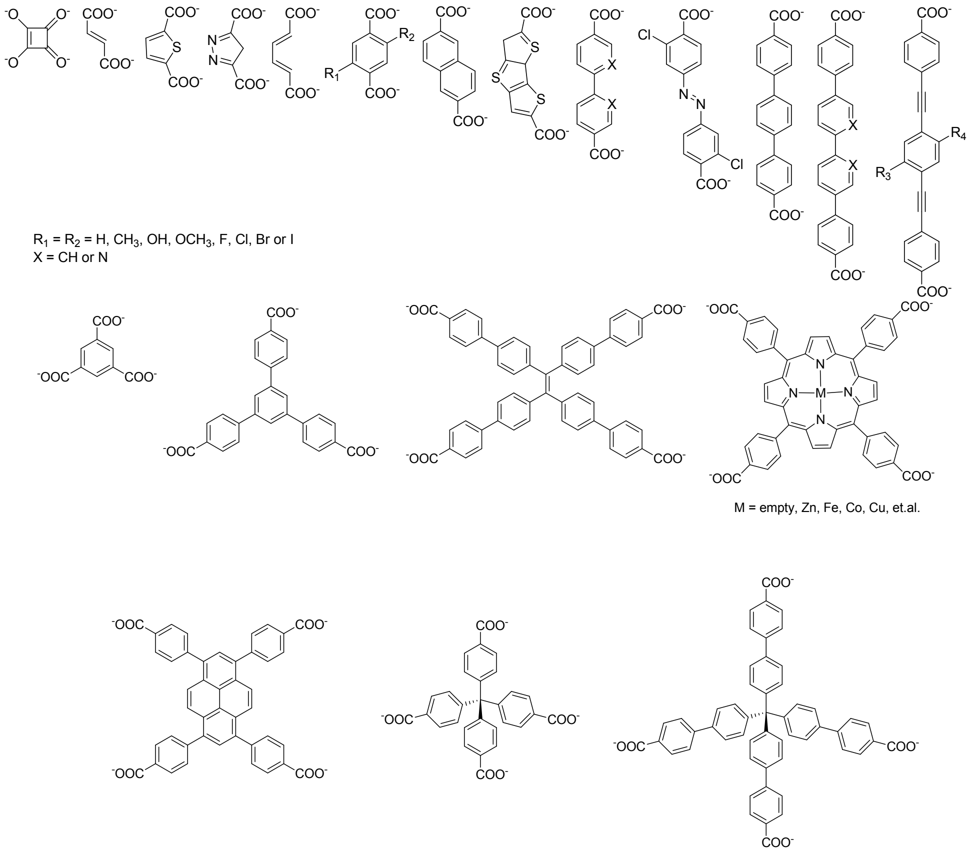

Figure S1. Summary of the multidentate carboxylate ligands incorporated into zirconium-based MOFs.

S2. Syntheses

All chemicals and solvents were purchased from commercial sources and were used as received without further purification.

S2.1. Single crystal ZrFA syntheses

A 21-mL glass vial was charged with $ZrCl_4$ (58 mg, 0.25 mmol; > 99.5 %, Sigma-Aldrich) and either 3,5-pyridinedicarboxylic acid (42 mg, 0.25 mmol) or 2,5-pyridinedicarboxylic acid (42 mg, 0.25 mmol). Thereafter, *N,N'*-dimethylformamide (4 mL; > 99.8 %, Ajax) and formic acid (7.5 mL; > 95 %, Sigma-Aldrich) were introduced. Colorless plate-like crystals were formed in the reaction medium following heating at 100 ^oC for 72 h.

S2.2. Powdered ZrFA syntheses

In a 21 mL glass vial, $ZrCl_4$ (58 mg, 0.25 mmol), DMF (4 mL) and formic acid (7.5 mL) were introduced. After sonication for 10 min, the obtained clear solution was heated at 100 ^oC for 16 h to obtain a microcrystalline powder ZrFA (60% yield, based on Zr).

S3. Single crystal X-ray diffraction

Data for ZrFA were collected on an Oxford Supernova diffractometer with Mo-Kα radiation (λ = 0.71073 Å) at 150 K. Empirical absorption corrections were made using SCALE3 ABSPACK.[19] Structure solutions were obtained by direct methods using SHELXS-97[20] and refined using SHELXL-97[21] in WinGX.[22] The hydrogen atoms were placed at calculated positions and refined as riding atoms with isotropic displacement parameters. CCDC 1023946 contains the supplementary crystallographic data for this paper. Data may be obtained free of charge via www.ccdc.cam.ac.uk/data_request/cif.

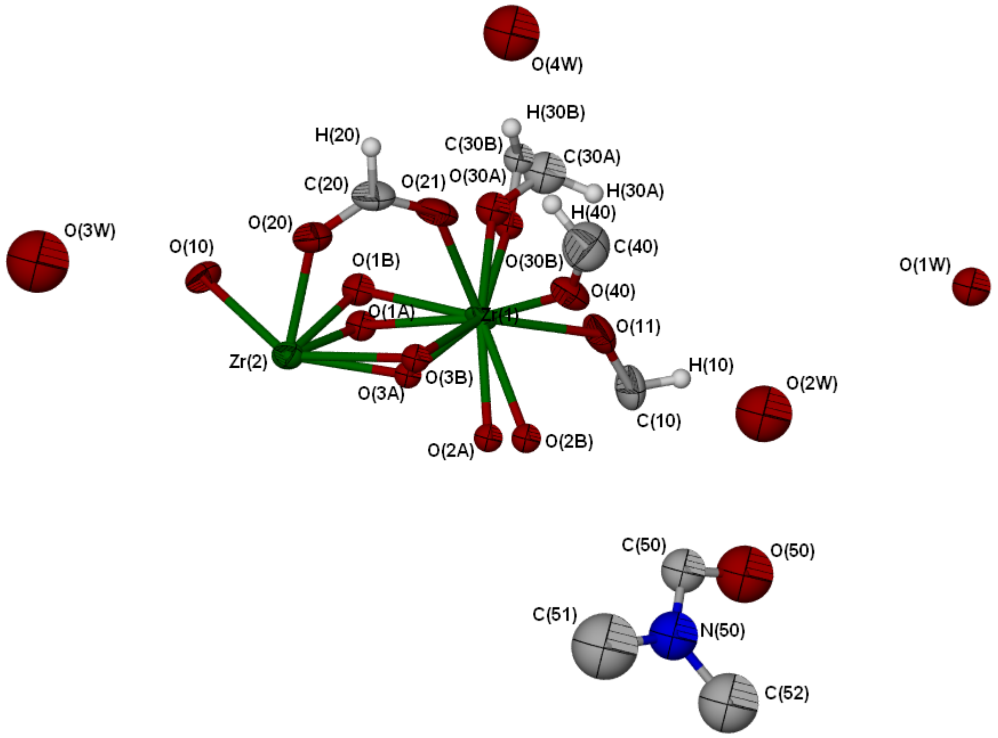

Figure S2. An ORTEP diagram of asymmetric unit of ZrFA. Atoms are shown as thermal ellipsoids at 50% probability.

Table S1. Single crystal X-ray diffraction collection summary for ZrFA

Formula weight	1377.58
Temperature / K	150(2)
Crystal system	orthorhombic
Space group	*Cmcm*
a / Å	10.04970(10)
b / Å	19.9849(3)
c / Å	19.7712(2)
α / °	90
β / °	90
γ / °	90
Volume / Å^3	3970.89(8)
Z	4
ρ_{calc} / mg mm^{-3}	2.304
F(000)	2644.0
Crystal dimensions / mm^3	0.05 × 0.04 × 0.02
Radiation	CuKα (λ = 1.54178)
2θ range for data collection	8.84 to 151.78°
Index ranges	$-12 \leq h \leq 12$, $-24 \leq k \leq 25$, $-24 \leq l \leq 24$
Reflections collected	35477
Independent reflections	2259 [Rint = 0.0467, Rsigma = 0.0165]
Data / restraints / parameters	2259 / 9 / 145
Goodness-of-fit on F^2	1.064
Final R indexes [I≥2σ (I)]	R1 = 0.0546, wR2 = 0.1687
Final R indexes [all data]	R1 = 0.0572, wR2 = 0.1729
Largest diff. peak / hole / e Å^3	2.31 / -1.21

S4. X-ray powder diffraction (XRPD)

XRPD measurements were performed over the 5-40° 2θ range with a 0.02° step size and 2° min^{-1} scan rate on a PANalytical X'Pert Pro diffractometer fitted with a solid-state PIXcel detector (45 kV, 40 mA, 1° divergence and anti-scatter slits, and 0.3 mm receiver and detector slits) using Cu-Kα (λ = 1.5406 Å) radiation. Profile fits were performed using the Le Bail extraction method in GSAS.

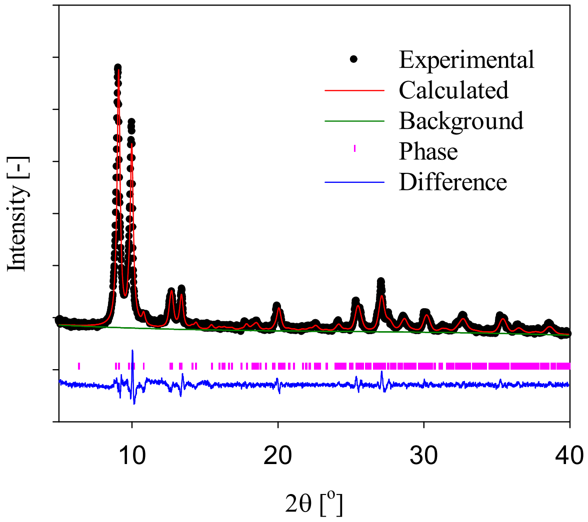

Figure S3. Le Bail refinement of ZrFA showing the experimental (black), calculated (red), background (green), and difference (blue). The positions of Bragg peaks are indicated by the pink bars.

S5. Variable temperature powder X-ray diffraction

VT-PXRD analysis of ZrFA was carried out using an Anton-Parr XRK900 vacuum furnace interfaced with a PANalytical X'pert Pro diffractometer using Cu-Kα radiation ($\lambda = 1.5406$ Å). Measurements were performed between 50 and 450 °C with a 20 °C temperature steps and a ramp rate of 5 °C.min^{-1}.

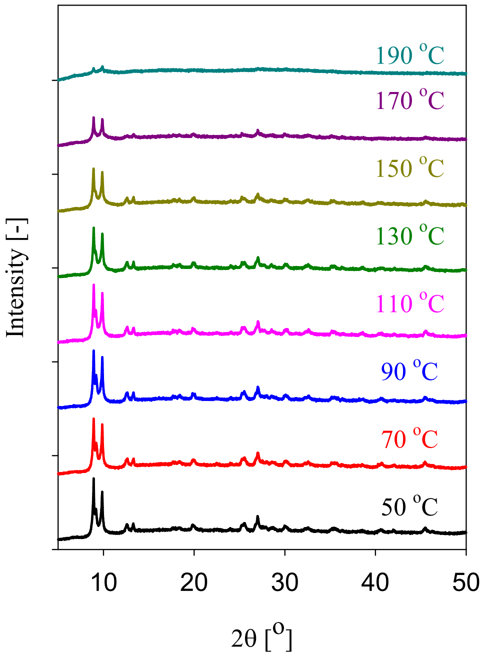

Figure S4. VTXRPD spectra for activated ZrFA.

S6. Thermogravimetric Analysis (TGA)

TGA analysis was performed on a TA Instruments Hi-Res TGA 2950 Thermogravimetric Analyser. Approximately 10 mg of sample was placed in a platinum pan which was heated under a flow of dry N_2 at a rate of 5 °C.min^{-1} up to 800 °C.

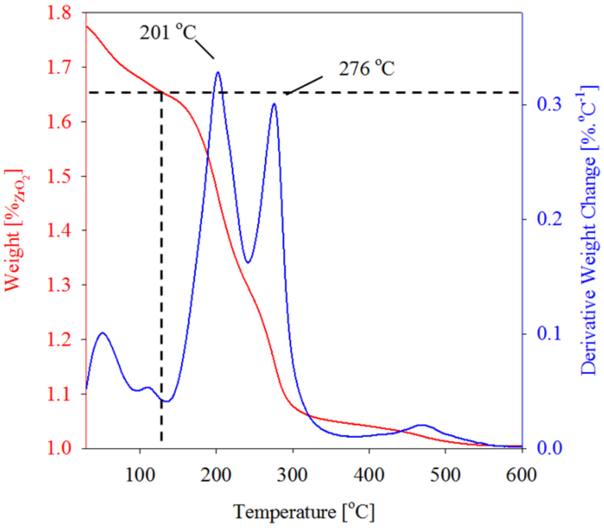

Figure S5. Weight change (red line) and derivative weight change (blue line) for activated ZrFA.

S7. Diffuse reflectance infrared spectra (DRIFTS)

DRIFTS were recorded for ZrFA on a Bruker Tensor 27 FTIR spectrometer in a KBr matrix.

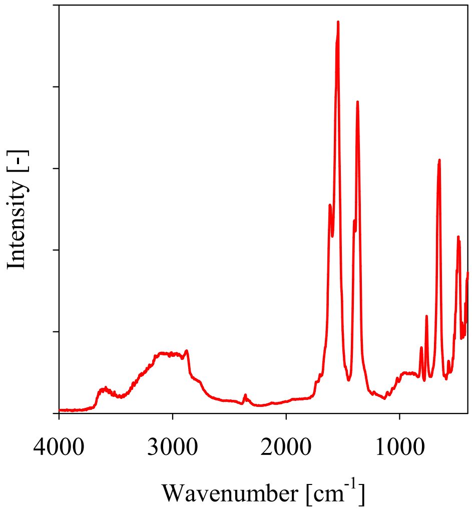

Figure S6. DRIFTS spectrum of activated ZrFA.

S8. Adsorption analysis

N_2 and CO_2 sorption isotherms were recorded on an Accelerated Surface Area & Porosimetry System, ASAP 2020 (Micromeritics Instruments Inc.). Prior to analysis, the materials were solvent exchanged with acetone using a soxhlet washing procedure for 12 h. Approximately 100 mg of the powdered solid was loaded into a glass analysis tube and outgassed for 12 h under dynamic vacuum (~ 10^{-6} bar) at 60 °C.

N_2 and CO_2 adsorption and desorption isotherms were measured at different temperatures (77, 293, 303, and 313 K for N_2 and 293, 303, and 313 K for CO_2).

Calculation of the CO_2 heat of adsorption involves the generation of an interpolated curve by spline fitting of data points using ASAP2020 software. This was used to fit data for CO_2 adsorption isotherms at 293, 303, and 313 K with the Clausius-Clapeyron equation which was used to determine the isosteric enthalpy of adsorption at specific surface coverage.

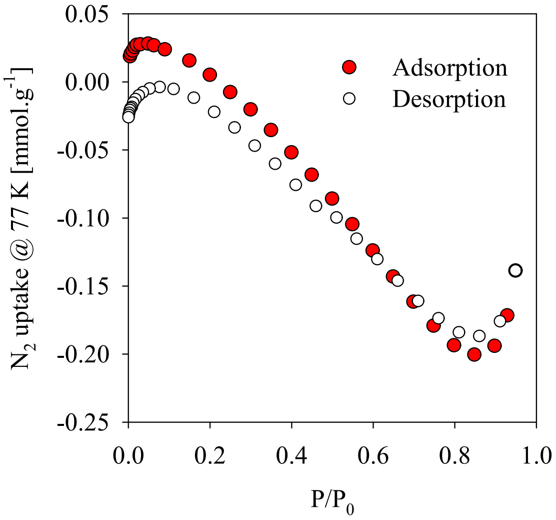

Figure S7. 77 K N_2 uptake isotherm for ZrFA.

S9. IAST calculations

A dual-site Langmuir-Freundlich (DSLF) equation:

$$N = N_A + N_B = \frac{N_{A,sat} k_A P^{n_A}}{1 + k_A P^{n_A}} + \frac{N_{B,sat} k_B P^{n_B}}{1 + k_B P^{n_B}}$$

was used to fit the adsorption isotherm of pure CO_2 and N_2 gas, where P is the pressure of bulk gas at equilibrium with adsorbed phase, N_i is maximum loading in site (i = A and B), k_i is the affinity constant, and n_i is used to characterize the deviation from the simple Langmuir equation. The fitted parameters will then used to predict the adsorption of mixture based on ideal-adsorbed solution theory (IAST).[23] There is no restriction on the choice of the model to fit the adsorption isotherm, but data over the pressure range under study should be fitted very precisely.

Table S2. Fitted parameters using the dual-site Langmuir-Freundlich (DSLF) equation

Zr_FA		$N_{i,A,sat}$ mol kg^{-1}	$N_{i,B,sat}$ mol kg^{-1}	$k_{i,A}$ mbar^{-1}	$k_{i,B}$ mbar^{-1}	$n_{i,A}$ dimensionless	$n_{i,B}$ dimensionless
293 K	CO_2	0.728	3.380	0.01541	0.00066	0.933	0.866
	N_2	0.3053	0.0798	0.00011	0.00156	1.160	-

S10. References

1. H. Furukawa, F. Gándara, Y.-B. Zhang, J. Jiang, W. L. Queen, M. R. Hudson and O. M. Yaghi, *J. Am. Chem. Soc.*, 2014, **136**, 4369-4381.
2. M. Zhang, Y.-P. Chen, M. Bosch, T. Gentle, III, K. Wang, D. Feng, Z. U. Wang and H.-C. Zhou, *Angew. Chem., Int. Ed.*, 2014, **53**, 815-818.
3. J. E. Mondloch, W. Bury, D. Fairen-Jimenez, S. Kwon, E. J. DeMarco, M. H. Weston, A. A. Sarjeant, S. T. Nguyen, P. C. Stair, R. Q. Snurr, O. K. Farha and J. T. Hupp, *J. Am. Chem. Soc.*, 2013, **135**, 10294-10297.
4. W. Liang, R. Babarao and D. M. D'Alessandro, *Inorg. Chem.*, 2013, **52**, 12878-12880.
5. D. Feng, Z. Y. Gu, J. R. Li, H. L. Jiang, Z. Wei and H. C. Zhou, *Angew. Chem., Int. Ed.*, 2012, **51**, 10307-10310.
6. W. Liang and D. M. D'Alessandro, *Chem. Commun.*, 2013, **49**, 3706-3708.
7. M. Kandiah, M. H. Nilsen, S. Usseglio, S. Jakobsen, U. Olsbye, M. Tilset, C. Larabi, E. A. Quadrelli, F. Bonino and K. P. Lillerud, *Chem. Mater.*, 2010, **22**, 6632-6640.
8. M. Kim and S. M. Cohen, *CrystEngComm*, 2012, **14**, 4096-4104.
9. L. Li, S. Tang, C. Wang, X. Lv, M. Jiang, H. Wu and X. Zhao, *Chem. Commun.*, 2014, **50**, 2304-2307.
10. S. Biswas, J. Zhang, Z. Li, Y. Y. Liu, M. Grzywa, L. Sun, D. Volkmer and P. Van Der Voort, *Dalton Trans.*, 2013, **42**, 4730-4737.
11. Q. Yang, V. Guillerm, F. Ragon, A. D. Wiersum, P. L. Llewellyn, C. Zhong, T. Devic, C. Serre and G. Maurin, *Chem. Commun.*, 2012, **48**, 9831-9833.
12. Q. Yang, A. D. Wiersum, P. L. Llewellyn, V. Guillerm, C. Serre and G. Maurin, *Chem. Commun.*, 2011, **47**, 9603-9605.
13. P. Xydias, I. Spanopoulos, E. Klontzas, G. E. Froudakis and P. N. Trikalitis, *Inorg. Chem.*, 2014, **53**, 679-681.
14. B. Wang, H. Huang, X.-L. Lv, Y. Xie, M. Li and J.-R. Li, *Inorg. Chem.*, 2014, **53**, 9254-9259.
15. D. Feng, W.-C. Chung, Z. Wei, Z.-Y. Gu, H.-L. Jiang, Y.-P. Chen, D. J. Darensbourg and H.-C. Zhou, *J. Am. Chem. Soc.*, 2013, **135**, 17105-17110.
16. V. Guillerm, S. Gross, C. Serre, T. Devic, M. Bauer and G. Férey, *Chem. Commun.*, 2010, **46**, 767-769.
17. R. Wang, Z. Wang, Y. Xu, F. Dai, L. Zhang and D. Sun, *Inorg. Chem.*, 2014, **53**, 7086-7088.
18. B. Bueken, H. Reinsch, N. Reimer, I. Stassen, F. Vermoortele, R. Ameloot, N. Stock, C. E. A. Kirschhock and D. De Vos, *Chem. Commun.*, 2014, **50**, 10055-10058.
19. SCALE3 ABSPACK: Empirical absorption correction CrysAlis Software package. Oxford Diffraction Ltd.
20. G. M. Sheldrick, *SHELXS-97. Program for crystal structure solution*, University of Göttingen, Germany, 1997.
21. G. M. Sheldrick, *SHELXL-97. Program for crystal structure refinement*, University of Göttingen, Germany, 1997.
22. L. J. Farrugia, *J. Appl. Crystallogr.*, 1999, **32**, 837-838.
23. Myers, A. L., and J. M. Prausnitz. *AIChE J.,* 1965, **11**, 121-127.